Transient thermal error modeling of a ball screw feed system

Dongxu Su
Yang Li
Wanhua Zhao (whzhao@mail.xjtu.edu.cn)
Xi'an Jiaotong University
Huijie Zhang

Research Article

Keywords: Ball screw, Feed drive system, Thermal error, Error modeling, FEM

Posted Date: June 7th, 2022

DOI: https://doi.org/10.21203/rs.3.rs-1665270/v1

Transient thermal error modeling of a ball screw feed system

Dongxu Su[1], Yang Li[1], Wanhua Zhao[1*], Huijie Zhang[2]

[1]State Key Laboratory for Manufacturing System Engineering, Xi'an Jiaotong University, Xi'an, Shaanxi 710054, P.R.China

[2]Collaborative Innovation Center of High-End Manufacturing Equipment in Xi'an Jiaotong University, Xi'an, Shaanxi 710054, P.R.China

*Corresponding Author/E-mail: whzhao@mail.xjtu.edu.cn

Abstract: The thermal behaviors of the ball screw feed system significantly affect the machining accuracy of the machine tool, which is widely valued by users and manufacturers. In the current ball screws thermal error models, the moving heat source at nuts is simplified to a fixed heat source to simplify the calculation, which can decrease the model's prediction accuracy. A novel thermal error modeling method for the ball screw feed system is proposed by this paper based on the FEM. In the proposed method, the moving heat source at the nut is loaded into the model by changing the grid distribution at different time steps. Meanwhile, a series of thermal experiments are carried out to collect the thermodynamic data with the machine tool's feed drive system operating at a different speed. And then the multi-objective optimization method is introduced to obtain the heat generated by the nuts and the convection coefficient between the air and the screw. The experimental results show that the thermal error of the ball screw feed system is different when the feed system runs in different intervals, even if the temperature rise at measuring points is the same. In the final, experiments under different conditions are carried out and the proposed model is accurate enough to predict the thermal error of the ball screw feed system.

keywords： Ball screw, Feed drive system, Thermal error, Error modeling, FEM

1. Introduction

With the increasing demand for machining accuracy and efficiency, the control of thermal error has been more and more valued by machine tool manufacturers and users[1]. Though the feed system with full closed-loop control has better thermal stability, the manufacturing cost of the machine tool will be significantly increased, due to the use of grating rulers. Therefore, the ball screw feed system with semi-closed loop control is still irreplaceable. When semi-closed loop control is adopted, the thermal deformation of the ball screw will directly decrease the machine tool's positioning accuracy, which can also cause the machining accuracy to decrease. Therefore, a thermal error model that can predict ball screw feed system thermal characteristics is essential to optimize its design to improve the machine tool's positioning accuracy. Meanwhile, the thermal error at different linear axis positions can also be calculated by the model and be compensated online to improve the stability of the machine tool's positioning accuracy.

At present, the thermal error modeling methods for machine tools mainly include database-based methods

and model-based methods[2, 3]. Recently, with the successful application of intelligent learning algorithms represented by neural networks in various fields, more and more scholars apply them in the modeling of machine tools' thermal error. The single-directional multi-layered neural networks with error back-propagation (MLP), radial basis function neural networks (RBF), and Kohonen networks were adopted by Rojek and Kowal et al. to establish the ball screw feed system thermal error model respectively. Experiments were performed to validate the accuracy of the neural network modeling method for the ball screw feed system and the prediction accuracy of the three neural network models was also compared[4]. A new inverse random model was proposed by Li and Sun et al. to predict thermal error. The randomness of influencing factors was taken into consideration by this model through the combination of stochastic theory, genetic algorithm, and radial basis function neural network (RBFNN) [5]. The model took the temperature values at the nut and the bearings as the input and was validated by the experiment under a single working condition. Liu and Yang et al.[6] also proposed an improved modeling method for the linear motor feed system's thermal error based on, which took advantage of the combination with the strong generalization performance and avoidance of overfitting of Bayesian neural networks. Elman neural networks (ENs) were employed by Yang and Xing [7] to carry out the thermal error modeling of the high precision feed system. The differential evolution (DE) algorithm was used to optimize the initial weights and thresholds of the ENs. The feeding system's thermal error is reduced from 1.73 to 0.88 μm with the online compensation. In addition to the neural networks, the multiple linear regression[8, 9], support vector machine(SVM) [10] and grey rough set theory [11] were also widely adopted in the feed system thermal error modeling [12]. Due to the difficulty of measuring the screw temperature distribution directly, the temperature at the nut and bearing where the data is easier to collect is taken as the input to the data-based model. However, when the nut is running at different intervals on the feed system, it may turn out the different thermal error, although the temperature rise at the measuring point is the same, which is caused by the different temperature distribution of the lead screw. In this case, the data-based model cannot predict the feed system thermal error accurately.

The model-based methods mainly include analytical and numerical models [13]. An analytical model was established by Shi and Ma et al. to predict the thermal error of the ball screw feed system based on thermodynamic parameters calibrated by the experiments [14]. Feng and Li et al. [15] proposed an analytical transient temperature model of the ball screw under the running and stationary states of the feed system respectively. And then the thermal error model can be established, which was validated by the cutting compensation experiments. Finite difference methods (FDM) and finite element methods (FEM) are currently

widely used numerical modeling methods for machine tool's thermal errors. The feed system thermal error was divided into two parts by Liu and Sun et al. including internal heat source induced error and environment temperature-induced error. And the linear regression method and finite difference methods were adopted respectively to establish thermal error models [16]. Monte Carlo (MC) simulation-integrated FEM method was used by Li and Zhao et al. to calculate the heat generated by the heat source of the feed system. And then a numerical model for thermal error of the lead screw was put forward based on FDM [17]. Mian and Fletcher et al.[18] established a thermal deformation calculation model of machine tools based on FEM, which was used to explore the influence of ambient temperature on its accuracy. Min and Jiang[19] developed an integrated thermal model with the aid of the FEM to analyze the temperature distribution of a ball screw feed drive system. The thermal contact resistance between the bearing and its housing was taken into consideration in this model. To estimate the thermal error of the ball screw system and the effectiveness of the air cooling system, thermal behavior models using FEM and a modified lumped capacitance method (MLCM) were developed separately by Zhu and Liu et al[20, 21], which was validated by three different work conditions[22]. The heat generated by the nut is a moving heat source in the feed system, which is difficult to be loaded in the simulation model accurately and is also one of the key factors to affect the accuracy of the thermal error model. In the above models, the moving heat source at the nut is simplified to the uniform heat flux loaded on the whole stroke, the position of which does not change with time anymore. Due to the boundary conditions being inconsistent with the actual situation, calculation errors can be induced.

A transient thermal error model of the ball screw feed system is developed by this paper to overcome the existing models' shortcomings based on the FEM. The loading of the moving heat source at the nut can be realized by changing the grid at each calculation time step in the proposed model. Meanwhile, the multi-objective optimization method is applied to obtain the heat generated by the nuts and the convection coefficient between air and the screw. The model is validated by the various working conditions of the feed system running at different intervals.

The structure of this paper is arranged as follows: The ball screw feed system thermal error model based on FEM is established in Section 2. Meanwhile, the method for loading the moving heat source at nut into the model is also introduced in Section 2. In Section 3, the calculation methods for the boundary conditions in the model are given. In Section 4, the heat generated by the nuts and convection coefficient between air and the screw is calculated based on the multi-objective optimization method, and a series of experiments under different conditions are conducted to validate the proposed model. In the final, the conclusions and prospects

of this study are introduced in Section 5.

2 Thermal error modeling of ball screw feed system

The lead screw can be simplified to a one-dimensional rod model, because of its large aspect ratio and simple symmetrical structure, as shown in the Fig.1. In this one-dimensional model, the heat q_1 and q_3 generated by the front and rear bearings are transferred into the screw along its radial direction. The heat q_2 generated at the nut is not only transmitted to the screw but also reciprocates along the axis of the screw at the speed of v. The convective heat transfer, with convective coefficient h, is conducted between the rest of the screw cylindrical surface and the air.

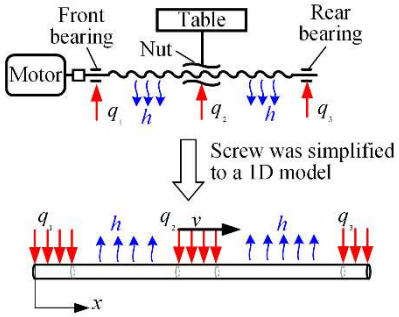

Fig.1. The one-dimensional model of the ball screw feed system

The simplified one-dimensional heat conduction equation of the ball screw is as follows,

$$k\frac{\partial^2 T(x,t)}{\partial x^2}=\rho c_p\frac{\partial T(x,t)}{\partial t} \tag{1}$$

The boundary conditions and initial conditions are written as,

$$B.C.\begin{cases}-k\dfrac{\partial T}{\partial n}=q_i & i=1,2,3 \quad on\ \Gamma_{qi}\\ -k\dfrac{\partial T}{\partial n}=h\left(T-T_{evn}\right) & on\ \Gamma_h\end{cases} \tag{2}$$

$$I.C. \quad T\left(x,0\right)=T_0 \quad at \quad t=0 \tag{3}$$

Where, k, ρ, *and* c_p are the thermal conductivity, density and specific heat capacity respectively, $T(x,t)$ is the temperature at the x position of the screw at time t and T_{evn} is the environmental temperature.

The analytical solution of the equation is difficult to be obtained, due to the loading position of the boundary condition q_2 of the model changing with time. Therefore, the numerical method is needed to solve the heat transfer equations. The FEM is applied in this paper to establish the prediction model of the screw

temperature, as it has higher solution accuracy and is more suitable for irregular collection areas than the FDM.

2.1 Screw temperature calculation model

The screw temperature field $T(x,t)$ can be approximated by,

$$\hat{T} = \sum_{i=1}^{n} N_i T_i \tag{4}$$

Where N_i is the shape function，n is the number of the element nodes and T_i is the time-dependent node temperature.

The following equation can be obtained by integrating equation (1) in a finite element based on the Galerkin Method.

$$\int_{\Omega_e} N_i \left[\frac{\partial}{\partial x}\left(k_x \frac{\partial \hat{T}}{\partial x} \right) - \rho c_p \frac{\partial \hat{T}}{\partial t} \right] d\Omega_e = 0 \tag{5}$$

The matrix form can be written as follows,

$$[\mathbf{C}]_e \left\{ \frac{d\mathbf{T}}{dt} \right\}_e + [\mathbf{K}]_e \{\mathbf{T}\}_e = \{\mathbf{f}\}_e \tag{6}$$

Two-node one-dimensional linear element is selected in the proposed model, as shown in Fig.2., the shape function of which can be expressed by,

$$N_i = 1 - \frac{x}{l}, N_j = \frac{x}{l} \tag{7}$$

The differential of the temperature function $T(x,t)$ to the space coordinate x be expressed as follows,

$$\frac{\partial T}{\partial x} = \frac{\partial N_i}{\partial x} T_i + \frac{\partial N_j}{\partial x} T_j = -\frac{1}{l} T_i + \frac{1}{l} T_j = [\mathbf{B}]_e [\mathbf{T}]_e \tag{8}$$

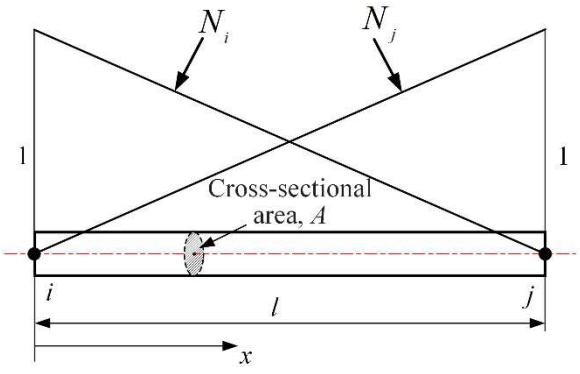

Fig.2. The two-node one-dimensional linear element

Then, the capacity matrix $[\mathbf{C}]_e$, stiffness matrix $[\mathbf{k}]_e$ and load vector $\{\mathbf{f}\}_e$ of each element can be calculated

as follows,

$$\begin{cases} [\mathbf{C}]_e = \int_\Omega (\rho c_p)[\mathbf{N}]_e^T [\mathbf{N}]_e \, d\Omega = \dfrac{\rho c_p l A}{6}\begin{bmatrix} 2 & 1 \\ 1 & 2 \end{bmatrix} \\ [\mathbf{k}]_e = \int_l [\mathbf{B}]^T [\mathbf{D}][\mathbf{B}] A dx + \int_{A_r} h[\mathbf{N}]^T [\mathbf{N}] dA_r = \dfrac{A k_x}{l}\begin{bmatrix} 1 & -1 \\ -1 & 1 \end{bmatrix} + \dfrac{hPl}{6}\begin{bmatrix} 2 & 1 \\ 1 & 2 \end{bmatrix} \\ \{\mathbf{f}\}_e = -\int_{A_s} q_i [\mathbf{N}]^T dA_s + \int_{A_s} hT_{evn} [\mathbf{N}]^T dA_s = -\dfrac{qPl}{2}\begin{Bmatrix} 1 \\ 1 \end{Bmatrix} + \dfrac{hT_{env}Pl}{2}\begin{Bmatrix} 1 \\ 1 \end{Bmatrix} \end{cases} \tag{9}$$

Where l is the length of the element, A and P is the area and perimeter of the element's cross-section.

The equation systems can be obtained by assembling the element matrix, as shown follows.

$$[\mathbf{C}]\left\{\frac{d\mathbf{T}}{dt}\right\} + [\mathbf{K}]\{\mathbf{T}\} = \{\mathbf{f}\} \tag{10}$$

The time term in the Equation (10) can be expressed as follows,

$$T^{n+\theta} = \theta T^{n+1} + (1-\theta)T^n \tag{11}$$

Then, the Equation (10) can be written as follows,

$$[\mathbf{C}]\left\{\frac{\mathbf{T}^{n+1} - \mathbf{T}^n}{\Delta t}\right\} + [\mathbf{K}]\left\{\theta \mathbf{T}^{\theta+1} + (1-\theta)\mathrm{T}^n\right\} = \theta\{\mathbf{f}\}^{n+1} + (1-\theta)\{\mathbf{f}\}^n \tag{12}$$

The above equation can be rearranged as follows,

$$([\mathbf{C}] + \theta\Delta t[\mathbf{K}])\{\mathbf{T}\}^{n+1} = ([\mathbf{C}] - (1-\theta)\Delta t[\mathbf{K}])\{\mathbf{T}\}^n + \Delta t\left(\theta\{\mathbf{f}\}^{n+1} + (1-\theta)\{\mathbf{f}\}^n\right) \tag{13}$$

The Backward difference method (θ=1) is applied in this paper to calculate the screw transient temperature field. The temperature distribution over the entire length of the screw can be calculated based on equation (13), after the initial conditions and thermal boundary conditions given.

2.2 Moving heat sources loading and thermal error modeling

The position of the heat source at the nut is also constantly changing along the screw axis when the feed system is running. This paper proposed a novel method to realize the loading of the moving heat source at the nut by changing the grid distribution on each time step.

The screw is divided into five parts along the axial direction as shown in Fig.3. where $x(t)$ is the position of the nut at different times， L_z is the width of the bearing, L_n is the width of the nut, and N_i (i=1,2,…,5)is the number of elements in each part. The different positions of the nut $x(t)$ can be calculated at each time step. And then the mesh of the model will be updated at the corresponding moment.

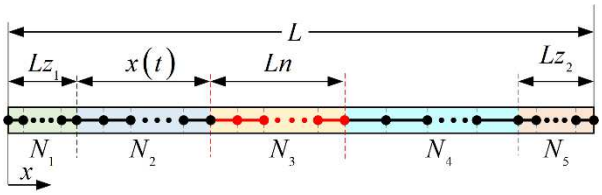

Fig.3. The meshing of the screw

First of all, the reciprocating motion of the screw in a certain interval is defined as the smallest unit of the screw's complex running trajectory to calculate $x(t)$ in the current time step which can be expressed by a work condition vector $\boldsymbol{a}=[p_1 \quad p_2 \quad v \quad t]^{\mathrm{T}}$, where p_1、p_2 、v 、t are the starting point, ending point, feed rate and running time respectively under the single work condition. Then, at time t, the position $x(t)$ of the nut on the screw can be written as follows,

$$x(t)=\begin{cases}\left[\text{floor}\left(\dfrac{v\cdot t}{p_2-p_1}\right)+1\right]\cdot\left(p_2-p_1\right)-v\cdot t+p_1 & \text{mod}\left[\text{floor}\left(\dfrac{v\cdot t}{p_2-p_1}\right),2\right]=1\\ v\cdot t-\text{floor}\left(\dfrac{v\cdot t}{p_2-p_1}\right)\cdot\left(p_2-p_1\right)+p_1 & \text{mod}\left[\text{floor}\left(\dfrac{v\cdot t}{p_2-p_1}\right),2\right]\neq 1\end{cases} \tag{14}$$

The loading of the moving heat source at the nut can be realized by adding the boundary condition values to the corresponding positions of the model based on the following equation.

$$\begin{cases}q_1 & \left\{\Gamma_{q1}\middle|0<x\le Lz\right\}\\ q_2 & \left\{\Gamma_{q2}\middle|x(t)\le x\le Ln+x(t)\right\}\\ q_3 & \left\{\Gamma_{q3}\middle|L-Lz\le x\le L\right\}\\ h_0[T-T_{evn}] & \left\{\Gamma_h\middle|other\right\}\end{cases} \tag{15}$$

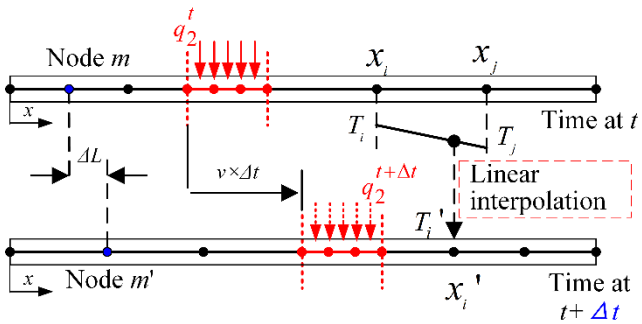

Fig.4. Node temperature transfer between adjacent time steps

The node temperature at the previous time step is required, when the backward difference method is adopted, as known in the equation (13). However, due to the position of the moving heat source changing, the position of the node also changes with the number of calculation steps increasing. Therefore, the linear interpolation method is introduced to obtain the previous node temperature, which is required to calculate the temperature

distribution at time t+Δt, as shown in Fig.4.

$$T_i' = T_i + \left(x_i' - x_i\right)\frac{T_j - T_i}{x_j - x_i} \tag{16}$$

As shown in Fig.5, the calculation process of the screw temperature field is as follows,

1)The initial temperature of the screw $T(x,0)$ will be given. And the time t is set to 0.

2） The position of the nut on the screw $x(t)$ at the time t can be calculated by equation (14). And then the mesh of the model can be updated.

3) The boundary conditions of the model can be calculated by equation (15). The screw temperature at time t_i can be solved after loading them into the model.

4) if t is less than the total running time t_{all}, t is accumulated by one-time step Δt and the process is returned to step 2). The position of the nut $x(t)$ will be recalculated. And the grid and the node temperature of the model will be also updated.

5) The above loop will repeat until t is equal to t_{all}.

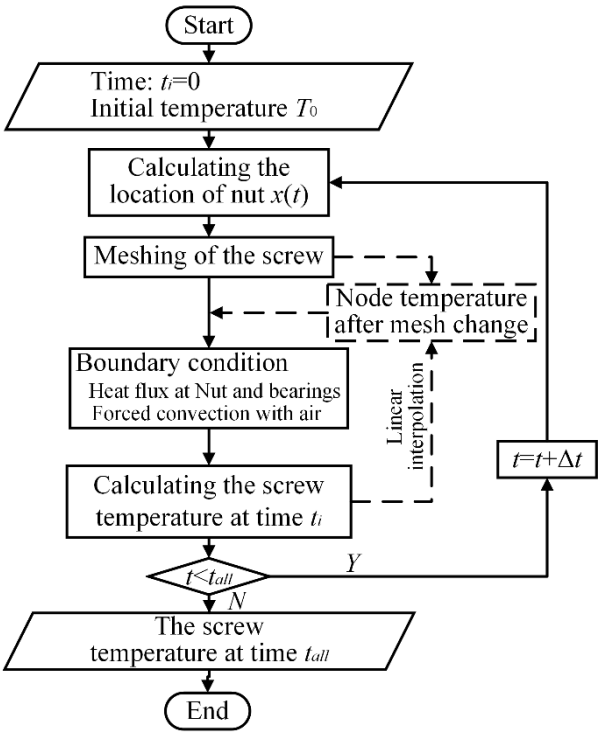

Fig.5. Screw temperature field calculation process

The complex working conditions of the feed system can be regarded as a combination of multiple single working condition, which can be expressed in the form of a matrix as follows.

$$A=\begin{bmatrix} p_{11} & p_{12} & \dots & p_{1n} \\ p_{21} & p_{22} & \dots & p_{2n} \\ v_1 & v_2 & \dots & v_n \\ t_1 & t_2 & \dots & t_n \end{bmatrix} \tag{17}$$

Each column in matrix **A** is a single working condition parameter. The screw temperature of the previous working condition is used as the initial condition for the calculation of the next working condition. And then the ball screw temperature field distribution under complex working conditions can be obtained.

Having the screw temperature obtained, the thermal error can be calculated as follows,

$$E(x,t)=\int_0^x \alpha T(x,t)dx \tag{18}$$

Where α is the thermal expansion coefficient.

3 Calculation of heat generation and heat dissipation

3.1 Heat generated by bearings

The bearing heating is caused by the friction loss and rolling resistance between the ball and the raceway in the contact area. An empirical formula for calculating bearing friction torque was proposed by Palmgren[23], which is composed of two parts, including the friction torque M_1 generated by the viscosity of the lubricant when the bearing is idling and the friction torque Mv generated by the load action independent of the speed.

$$M_1 = f_1 F_\beta d_m \tag{19}$$

$$M_v = \begin{cases} 10^{-7} f_0 (\upsilon_0 n)^{2/3} d_m^3 & vn \geq 2000 \\ 160\times 10^{-7} f_0 {d_m}^3 & vn < 2000 \end{cases} \tag{20}$$

The bearing heating is related to the friction torque of the contact area and rotation speed, which can be calculated as follows,

$$H_{bearing} = 1.047\times 10^{-4} \times \omega \left(M_1 + M_v \right) \tag{21}$$

3.2 Heat generated by nuts

Similar to the bearing heating, the heat generated by the screw nut pair is mainly caused by the friction between the ball and the nut groove, which can be expressed as follows,

$$H_{nut} = 0.12\pi nM \tag{22}$$

$$\begin{cases} M = M_a + M_b \\ M_a = \dfrac{F_{a1} \cdot P_h}{2\pi\eta}(1-\eta) \\ M_b = \dfrac{F_{a0} \cdot P_h}{2\pi\eta}(1-\eta^2) \end{cases} \tag{23}$$

Where n is screw rotation speed, M is the total friction torque, M_a is the torque that overcomes axial force and cutting force, M_b is the sum of resistance torque, F_{a1} is the axial force loaded on the nut, F_{a0} is the nut preload, P_h is the lead of screw and η is transmission efficiency.

3.3 Heat dissipation calculation

When the feed system is running, the screw surface is in full contact with the air and the air is forced to flow, due to the thread groove. The forced convection will be conducted between the screw surface and air. According to the Nusselt criterion, the convective coefficient can be expressed as follows,

$$h = \frac{N_u \cdot \lambda_f}{L} \tag{24}$$

Where N_u is the Nusselt number, λ_f is the thermal conductivity of the air and L is the hydraulic diameter。

The Nusselt number can be calculated as follows[24],

$$\begin{cases} Nu = 0.664\,\mathrm{Re}^{1/2}\,\mathrm{Pr}^{1/2} & \mathrm{Re} \le 43000 \\ Nu = 0.037\,\mathrm{Re}^{4/5}\,\mathrm{Pr}^{1/3} & \mathrm{Re} > 43000 \end{cases} \tag{25}$$

4. Experimental validations

4.1 Experimental setup and testing results

A series of experiments were carried out on the X-axis ball screw semi-closed loop feed system of a gantry milling machine in this paper, as shown in Fig.6. The 7006C/DF angular contact ball bearings with back-to-back installed were selected as the front bearing of the screw. The rear bearing on the screw was the 61906 deep groove ball bearing.

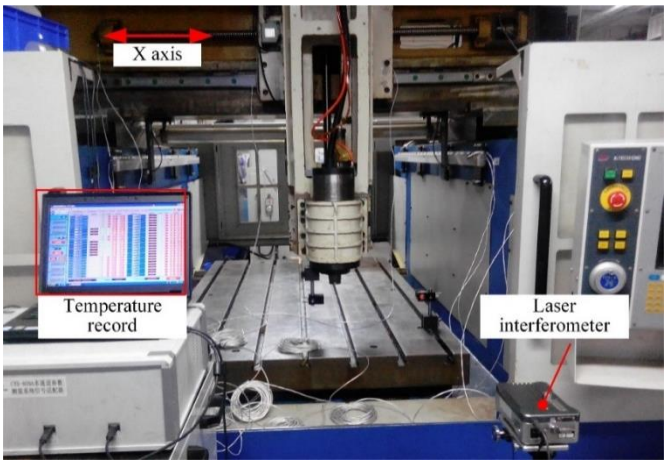

Fig.6. Photograph of the experimental setup

The dimensional parameters and material properties of the screw are given in Table 1 and Table 2 respectively.

Table 1. Dimensional parameters of the screw

Length of screw /mm	Diameter /mm	Starting position /mm	Ending position /mm	Length of nut /mm	Screw lead /mm
1800	37	460	1260	120	12

Table 2. Screw material properties

Density /kg·m^{-3}	Young's modulus /Gpa	Specific heat capacity /J·kg^{-1}·k^{-1}	Thermal Conductivity /w·m^{-1}·k^{-1}	Expansion coefficient / μm·m^{-1}·k^{-1}
7850	200	448	70	12

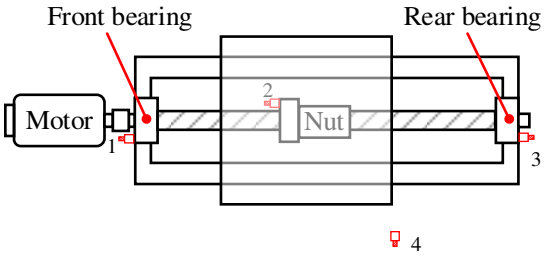

Fig.7. Thermal sensor layout

As shown in Fig.7, four thermal sensors were arranged around the feed system to measure the front/rear bearing, nuts and environment temperature. Meanwhile, the laser interferometer was adopted to measure the positioning accuracy of the feed system at different times, and then the thermal error can be calculated.

The temperature rise at each test point is shown in Fig.8. when the feed system run according to the work conditions in Table 3.

Table 3. Experimental work conditions

Work condition No.	1	2	3	4
Running interval /mm	0~200	0~300	400~600	400~800
Feed rate/ m·min^{-1}	5.4			
Running time/h	3			

During the test, the environmental temperature changed within 1℃, the influence of which on the positioning accuracy can be ignored. The feed system can reach the thermal steady state after running for three hours. The temperature rise at the front bearing house is the highest, which is closed to 3℃. While, the temperature rise at the nut is the lowest, around 2 ℃ revealed in Fig.8.

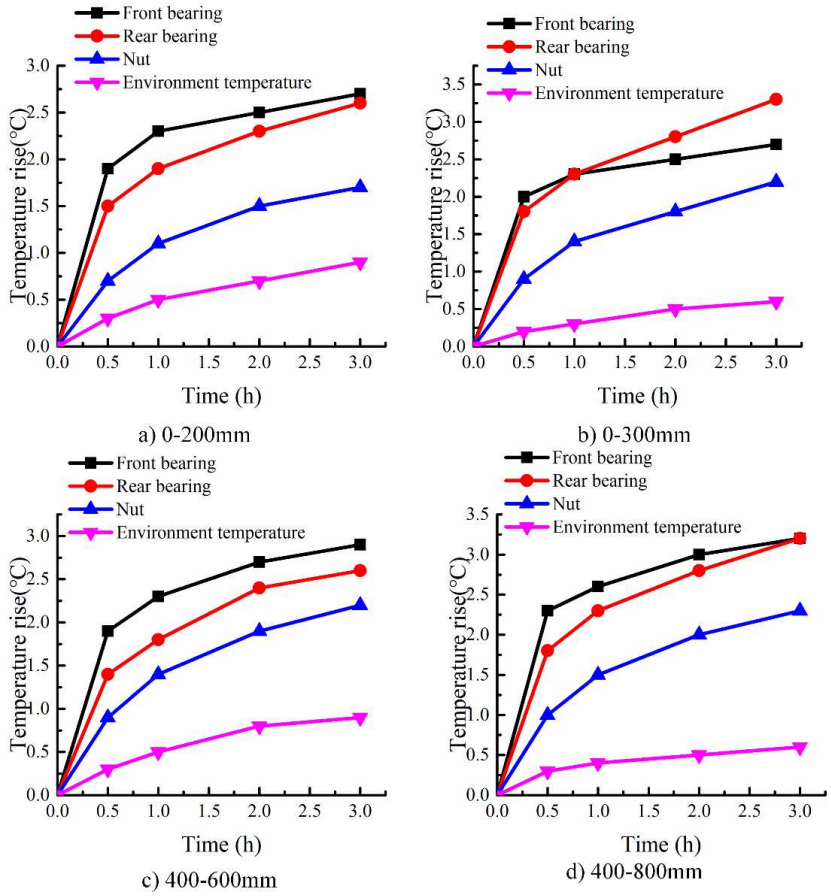

Fig.8. Temperature rise under different working conditions

The Fig.9 shows the thermal error of the feed system under different work conditions. When the feed system runs under different work conditions, although the temperature rise at the measuring point is roughly the same, the positioning error is completely different. As shown in Fig.9 (a) and (b), when the nut runs on the front half

of the screw (0-200mm and 0-300mm), thermal error at end of the screw can reach 10~15μm. The thermal extension of the screw is larger on the front half of the screw. So the thermal error tends to be concave-down along the axial direction. While the changing trend of thermal error is the opposite when the nut is running on the rear half of the screw (400-600mm and 400-800mm) as shown in Fig.9 (c) and (d). The maximum thermal error can reach around 20μm under work condition 3 and 4.

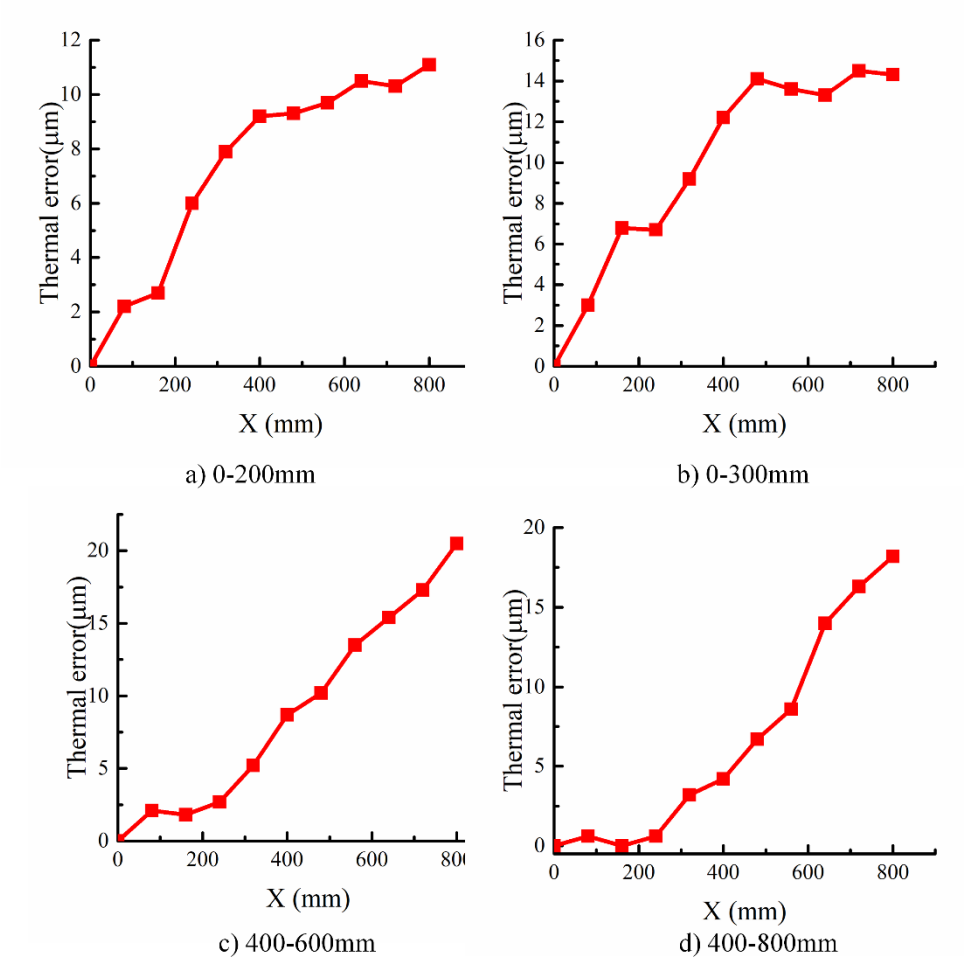

Fig.9. Thermal error under different work conditions

4.2 Model parameter identification

The accuracy of the boundary condition value is one of the key factors to ensure the accuracy of the thermal model. However, the convective coefficient between the screw surface and its surrounding air is difficult to be accurately calculated with simple empirical formulas, due to the thread grooves on the screw surface. In addition, the heat generated by nut is also difficult to be accurately expressed based on the simple empirical formula, because it can be affected by various factors such as preload, abrasion et al. Therefore, the parameter identification method was adopted by this paper to calculate the convective coefficient and the heat generated

by the nut based on the experimental data of the above work conditions.

As shown in Fig.10, the mean square error (MSE) of the simulated value and the experimental value was applied to construct the objective function, which can be expressed as follows,

$$\min \ mse_i = \sum_{k=1}^{m} \left[\varepsilon_e(k) - \varepsilon_{sim}(k) \right]^2 \Big/ (m-1) \qquad i = 1,2,3,4 \tag{26}$$

Where mse_i is the MSE under the i_{th} working condition， m is the total number of samples， $\varepsilon_e(k)$ is experimental thermal error at the k_{th} sampling， $\varepsilon_{sim}(k)$ is the simulated thermal error at the k_{th} sampling.

The convective coefficient h and the heat generated by nut q_2 were taken as the optimized variables. To improve computational efficiency, 50 Design Points of Experiments (DOE), within the range of $50 \le h \le 60, 690 \le q_2 \le 720$, are generated through the Optimal Latin Hypercubes (OLHCs) method[25]. And then a mapping model between optimized variables and objective functions was established based on the moving least squares method[26] (MLS) to replace the original FE model. In the final, the Pareto front of h and q_2 was obtained by the multi-objective optimization method, as shown in Fig.11.

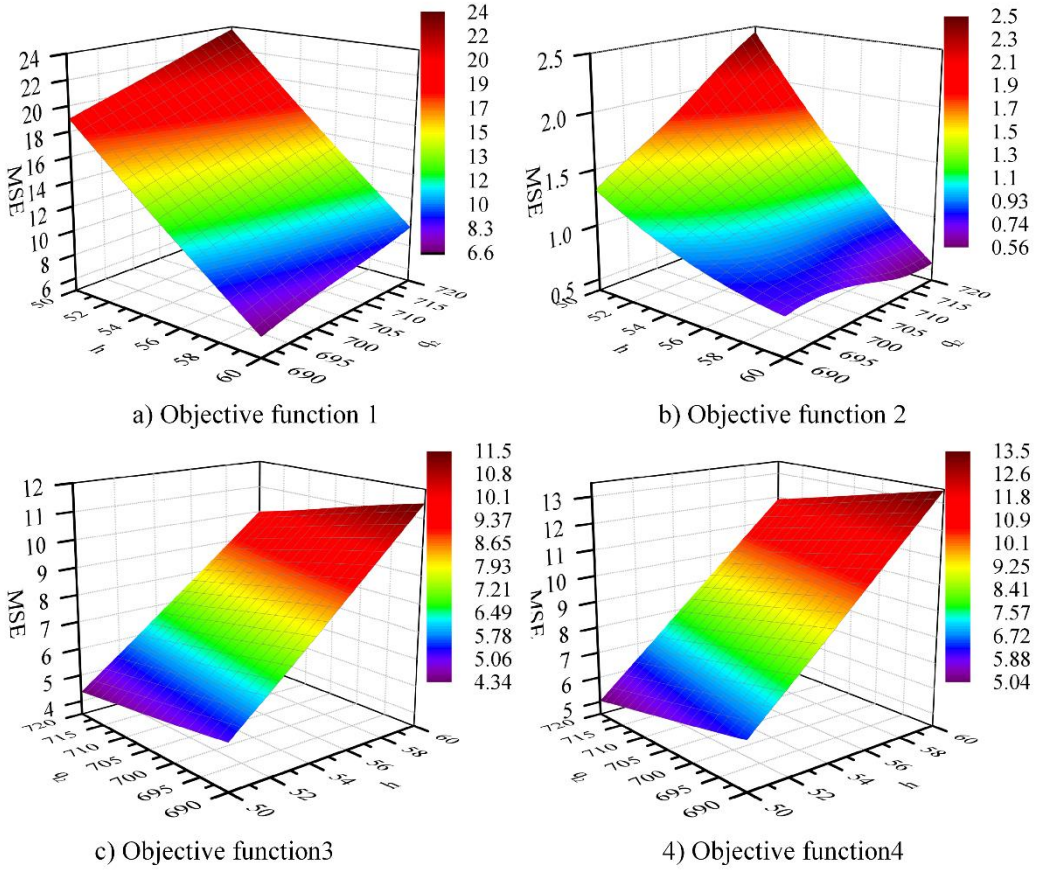

Fig.10. Objective function

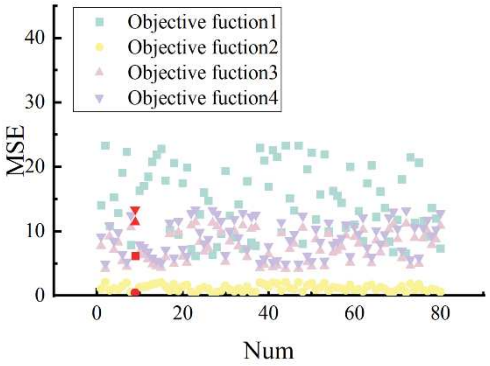

Fig.11. Optimal solution selection

The boundary condition values in the model are listed in the Table 4.

Table 4. The value of boundary conditions

Boundary conditions	Values
q_1/W·m^{-2}	1332.5
q_2/W·m^{-2}	690
q_3/W·m^{-2}	1200
h_0/W·m^{-2}·k^{-1}	59.5

4.3 Validations under different operating conditions

The feed system run according to the different work conditions as listed in the Table 5 and 6 to validate the proposed model.

Table 5. Single work condition to validate the model

Work condition No.	5	6	7
Running interval /mm	0~600	200~400	200~600
Feed rate / m·min^{-1}		5.4	
Running time /h		3	

According to the working condition listed in the Table 5, the experimental thermal error value and the simulated value obtained by the proposed method are shown in Fig.12. When the feed system runs under work condition 5, the maximum thermal error of the feed system can reach up to 14μm. The maximum prediction error of the proposed model is less than -4μm. The maximum thermal error of the feed system under work condition 6 is nearly 14μm. The model's prediction error is within 5μm, as shown in Fig.12 (b). According to the Fig.12 (c), the prediction error of the model also is within 4μm, when the feed system run with work condition 7.

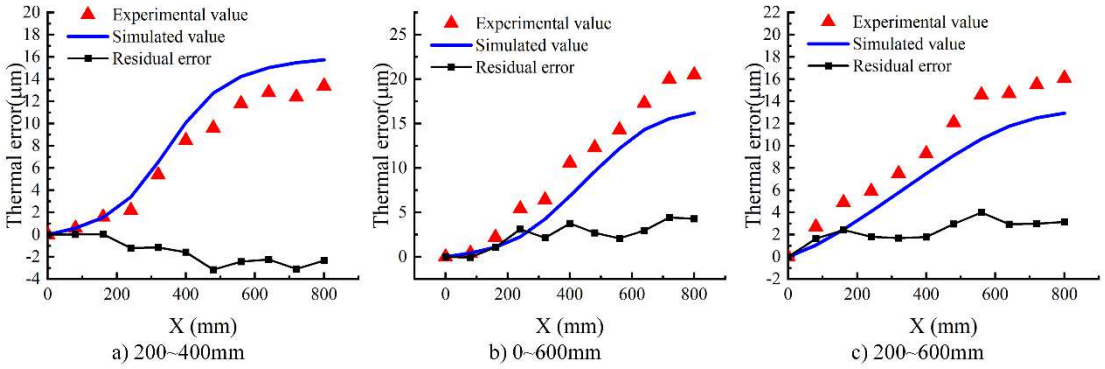

Fig.12. The experimental and simulated value of thermal error under working conditions 5~7

Table 6. Combined work conditions to validate the model

Work condition No.	Running interval 1/ mm	Running interval 2/ mm	Running interval 3/ mm
8	0～300	500～800	200～600
9	100～600	300～400	200～700

According to the working conditions listed in Table 6, the feed system run at the feed speed of 0.09 m/s for 0.5 hours in each interval. The laser interferometer was used to collect thermal error every 0.5 hours. The matrix $\mathbf{A_1}$ and $\mathbf{A_2}$ are respectively used as the input of the proposed model, and the simulated value of the thermal error would be obtained in the final.

$$\mathbf{A_1}=\begin{bmatrix} 0.0 & 0.5 & 0.2 \\ 0.3 & 0.8 & 0.6 \\ 0.09 & 0.09 & 0.09 \\ 1800 & 1800 & 1800 \end{bmatrix}, \mathbf{A_2}=\begin{bmatrix} 0.1 & 0.3 & 0.2 \\ 0.6 & 0.4 & 0.7 \\ 0.09 & 0.09 & 0.09 \\ 1800 & 1800 & 1800 \end{bmatrix} \quad (27)$$

As shown in Fig.13, when the feed system run under work condition 8, the maximum thermal error varies between 11μm-18μm. At 0.5h, 1.0h and 1.5h, the prediction errors of the proposed model are 0~-3μm, -2~+2μm and 0~2μm respectively.

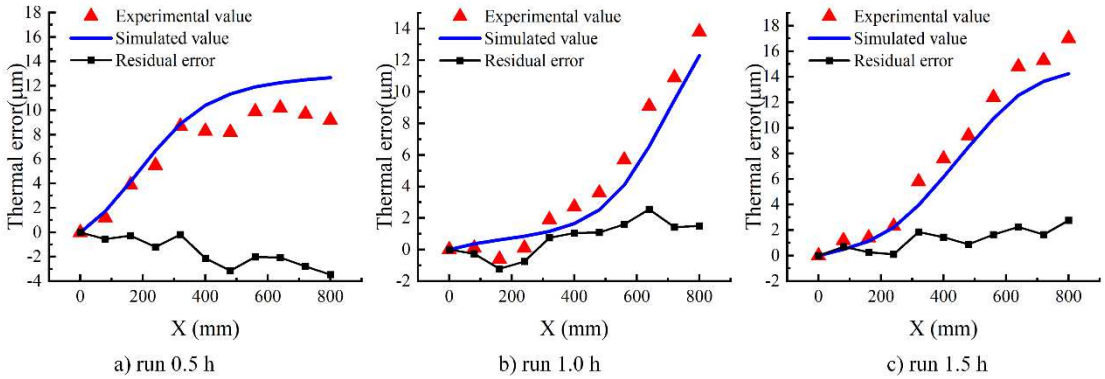

Fig.13. The experimental and simulated value of thermal error under working condition 8

The Fig.14 shows that the maximum thermal error of the feed system varies from 14μm to 20μm with running under work condition 9. And the prediction errors of the proposed model are -2~+2μm，-2~+1μm and 0~5μm respectively.

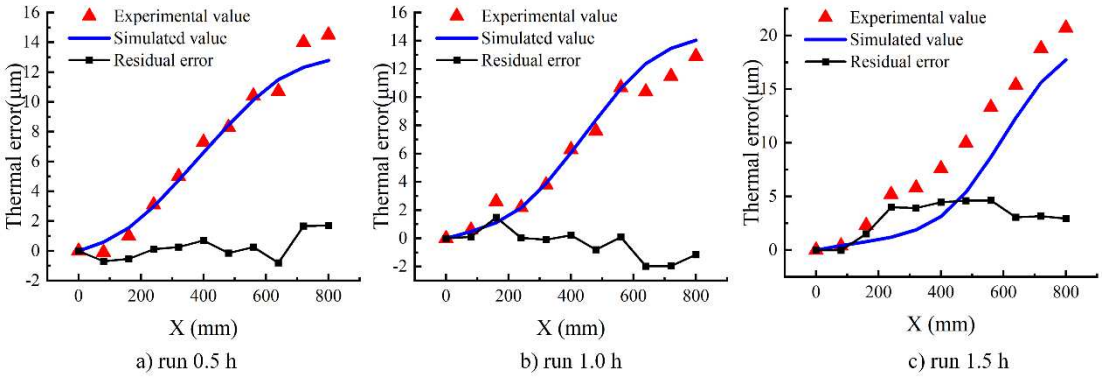

Fig.14. The experimental and simulated value of thermal error under working condition 9

To sum up, the ball screw feed system thermal error model proposed in this paper has high accuracy under various working conditions, the prediction of which is within 5μm. As shown in Fig.12(b) and Fig.14(c), the prediction accuracy of the model decreases, when the feed system is running on a larger stroke. And the predicted value is lower than the actual measured value, which may be caused by the actual heat generation increasing with the time increasing, because the lubrication status gets worse in the case of large stroke running.

5. Conclusion

A transient thermal error model of the ball screw feed system was developed in this paper based on FEM. The loading of the moving heat source at the nut on the model was realized by changing the grid of the model at each time step to predict the thermal error of the feed system under complex work conditions. In addition, the multi-objective optimization method was applied in this paper to calibrate the value of boundary conditions loaded on the proposed model to improve the accuracy of the model, because of the difficulty to calculate the convection coefficient and the heat generated by the nut accurately. The core conclusions of the study are as follows:

(1) Under different work conditions, even if the temperature rises at the measuring point are approximately close, the thermal errors of the feed system can also be completely different due to the difference in the screw temperature distribution.

(2) The proposed model is reliable and accurate to predict the transient thermal error of the ball screw feed system under different work conditions, the prediction error of which was controlled within 5μm.

In further investigations, the change of the heat generated by the nut during the feed system running needs to be taken into consideration to improve the accuracy of the model. In addition, the proposed model can be further embedded in the NC system and compensate the thermal error online to improve the stability of the machine tool's positioning accuracy.

Acknowledgments

This work was financially supported by the Key-Area Research and Development Program of Guangdong Province (Grant No. 2020B090927002). The first author would like to thank the China Scholarship Council (CSC) for financial support and the scholarship award.

Declarations

Funding: This work was financially supported by the Key-Area Research and Development Program of Guangdong Province (Grant No. 2020B090927002).

Competing interests: The authors declare that they have no known competing financial interests or personal relationships that could have appeared to influence the work reported in this paper.

Availability of data and materials: All data generated or analyzed during this study are included

Code availability: Not applicable.

Ethical approval: Not applicable.

Consent to participate: Not applicable.

Consent to publish: The authors consent that the work entitled as "Transient thermal error modeling of a ball screw feed system" for possible publication in International Journal of Advanced Manufacturing Technology. The authors certify that this manuscript is original and has not been published in whole or in part nor is it being considered for publication elsewhere.

Authors contributions: D. Su: Methodology, Data curation, Formal analysis, Writing – original draft, review & editing; Y. Li: Conceptualization, Supervision, Funding acquisition, Writing – review & editing; W. Zhao: Conceptualization, Supervision, Writing – review & editing; H. Zhang: Data curation, Validation, Writing – review & editing.

Reference

[1] Putz M, Richter C, Regel J, Bräunig M. (2018) Industrial consideration of thermal issues in machine tools. Production Engineering,12:723-736. doi: 10.1007/s11740-018-0848-6

[2] Brecher C, Ihlenfeldt S, Neus S, Steinert A, Galant A. (2019) Thermal condition monitoring of a motorized milling spindle. Production Engineering,13:539-546. doi: 10.1007/s11740-019-00905-3

[3] Mayr J, Jedrzejewski J, Uhlmann E, Alkan Donmez M, Knapp W, Härtig F, Wendt K, et al. (2012) Thermal issues in machine tools. CIRP Annals,61:771-791. doi: 10.1016/j.cirp.2012.05.008

[4] Rojek I KMSA. (2017) Predictive compensation of thermal deformations of ball screws in CNC machines using neural networks. Tehnicki vjesnik - Technical Gazette,24. doi: 10.17559/TV-20161207171012

[5] Li T, Sun T, Zhang Y, Zhao C. (2021) Prediction of thermal error for feed system of machine tools based on random radial basis function neural network. The International Journal of Advanced Manufacturing Technology,114:1545-1553. doi: 10.1007/s00170-021-06899-6

[6] Liu S, Yang Z, Wei Q, Chen Y, Liu L. (2021) Thermal Error Model of Linear Motor Feed System Based on Bayesian Neural Network. IEEE Access,9:112561-112572. doi: 10.1109/ACCESS.2021.3103972

[7] Yang H, Xing R, Du F. (2020) Thermal error modelling for a high-precision feed system in varying conditions based on an improved Elman network. The International Journal of Advanced Manufacturing Technology,106:279-288. doi: 10.1007/s00170-019-04605-1

[8] Ye W, Guo Y, Zhou H, Liang R, Chen W. (2020) Thermal error regression modeling of the real-time deformation coefficient of the moving shaft of a gantry milling machine. Advances in Manufacturing,8:119-132. doi: 10.1007/s40436-020-00293-3

[9] Shi H, Zhang D, Yang J, Ma C, Mei X, Gong G. (2016) Experiment-based thermal error modeling method for dual ball screw feed system of precision machine tool. The International Journal of Advanced Manufacturing Technology,82:1693-1705. doi: 10.1007/s00170-015-7491-6

[10] Miao E, Gong Y, Niu P, Ji C, Chen H. (2013) Robustness of thermal error compensation modeling models of CNC machine tools. The International Journal of Advanced Manufacturing Technology,69:2593-2603. doi: 10.1007/s00170-013-5229-x

[11] Cheng Q, Qi Z, Zhang G, Zhao Y, Sun B, Gu P. (2016) Robust modelling and prediction of thermally induced positional error based on grey rough set theory and neural networks. The International Journal of Advanced Manufacturing Technology,83:753-764. doi: 10.1007/s00170-015-7556-6

[12] Pahk H, Lee SW. (2002) Thermal Error Measurement and Real Time Compensation System for the CNC Machine Tools Incorporating the Spindle Thermal Error and the Feed Axis Thermal Error. International journal of advanced manufacturing technology,20:487-494. doi: 10.1007/s001700200182

[13] Li Y, Zhao W, Lan S, Ni J, Wu W, Lu B. (2015) A review on spindle thermal error compensation in machine tools. International Journal of Machine Tools and Manufacture,95:20-38. doi: 10.1016/j.ijmachtools.2015.04.008

[14] Shi H, Ma C, Yang J, Zhao L, Mei X, Gong G. (2015) Investigation into effect of thermal expansion on thermally induced error of ball screw feed drive system of precision machine tools. International Journal of Machine Tools and Manufacture,97:60-71. doi: 10.1016/j.ijmachtools.2015.07.003

[15] Feng W, Li Z, Gu Q, Yang J. (2015) Thermally induced positioning error modelling and compensation based on thermal characteristic analysis. International Journal of Machine Tools and Manufacture,93:26-36. doi: 10.1016/j.ijmachtools.2015.03.006

[16] Liu K, Sun M, Wu Y, Zhu T. (2015) Thermal Error Modeling Method for a CNC Machine Tool Feed Drive System. Mathematical Problems in Engineering,2015:1-6. doi: 10.1155/2015/436717

[17] Li Z, Zhao C, Lu Z. (2020) Thermal error modeling method for ball screw feed system of CNC machine tools

in x-axis. The International Journal of Advanced Manufacturing Technology,106:5383-5392. doi: 10.1007/s00170-020-05047-w

[18] Mian NS, Fletcher S, Longstaff AP, Myers A. (2013) Efficient estimation by FEA of machine tool distortion due to environmental temperature perturbations. Precision Engineering,37:372-379. doi: 10.1016/j.precisioneng.2012.10.006

[19] Min X, Jiang S. (2011) A thermal model of a ball screw feed drive system for a machine tool. Proceedings of the Institution of Mechanical Engineers, Part C: Journal of Mechanical Engineering Science,225:186-193. doi:

[20] Xu Z, Choi C, Liang L, Li D, Lyu S. (2015) Study on a novel thermal error compensation system for high-precision ball screw feed drive (1st report: Model, calculation and simulation). International Journal of Precision Engineering and Manufacturing,16:2005-2011. doi: 10.1007/s12541-015-0261-4

[21] Xu ZZ, Liu XJ, Kim HK, Shin JH, Lyu SK. (2011) Thermal error forecast and performance evaluation for an air-cooling ball screw system. International Journal of Machine Tools and Manufacture,51:605-611. doi: 10.1016/j.ijmachtools.2011.04.001

[22] Xu Z, Choi C, Liang L, Li D, Lyu S. (2015) Study on a novel thermal error compensation system for high-precision ball screw feed drive (2nd report: Experimental verification). International Journal of Precision Engineering and Manufacturing,16:2139-2145. doi: 10.1007/s12541-015-0276-x

[23] Palmgren A. (1959) Ball and roller bearing engineering. Philadelphia: SKF Industries Inc. doi:

[24] Uhlmann E, Hu J. (2012) Thermal Modelling of a High Speed Motor Spindle. Procedia CIRP,1:313-318. doi: 10.1016/j.procir.2012.04.056

[25] Gilkeson CA, Toropov VV, Thompson HM, Wilson M, Foxley NA, Gaskell PH. (2014) Dealing with numerical noise in CFD-based design optimization. Computers & Fluids,94:84-97. doi:

[26] Lancaster P, Salkauskas K. (1981) Surfaces generated by moving least squares methods. Mathematics of computation,37:141-158. doi: